INFLUENCE OF A SKIN EFFECT IN THE SQUIRREL CAGE ON A SPEED-TORQUE CHARACTERISTICS OF THE INDUCTION MOTOR

Radoslav Cipín
Doctoral Degree Programme (1), FEEC BUT
E-mail: xcipin00@stud.feec.vutbr.cz

Josef Běloušek
Doctoral Degree Programme (3), FEEC BUT
E-mail: xbelou00@stud.feec.vutbr.cz

Supervised by: Miroslav Patočka
E-mail: patocka@feec.vutbr.cz

ABSTRACT

The article deals with the influence of skin effect in the squirrel cage of the induction motor (IM) on a speed-torque characteristics. The equivalent circuit of IM is taken in the shape of the Γ-circuit, not the T-circuit. The skin effect calculations are given under the assumption that the cross-section of the rotor bar is rectangular. For that bar are calculated a frequency dependence of rotor resistance and leakage inductance. The theoretical results are compared with measured values.

1. INTRODUCTION

It is well known that parameters (i. e. resistances, inductances) of induction motor are not constant during its running, for example stator and rotor resistance is depended on temperature. In this article is shown the dependence of the skin effect in the IM squirrel cage on a speed-torque characteristics.

2. THE EQUIVALENT CIRCUIT OF A INDUCTION MOTOR

The equivalent circuit of one phase of IM is taken in the shape of the Γ-circuit according to Fig. 1. The exact transformation of the Γ-circuit on the T-circuit, including physical reasons, are introduced in [1], identical results are given in [2].

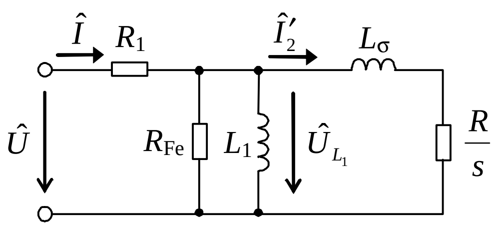

Fig. 1 The equivalent circuit of one phase of IM in the shape of the Γ-circuit**.**

Meanings of individual parameters:

$\hat{U}$ [V] stator voltage, $\hat{U}_{L_1}$ [V] voltage on stator inductance, $\hat{I}$ [A] stator current, $\hat{I}_2'$ [A] referred rotor current, R_1 [Ω] stator resistance, R_{Fe} [Ω] iron-loss resistance, R [Ω] rotor resistance transformed on stator, L_1 [H] stator inductance, L_σ [H] leakage inductance transformed on stator, s [-] slip.

2.1. THE SPEED-TORQUE CHARACTERISTICS OF INDUCTION MOTOR

The speed-torque characteristics of the induction motor is derived in a classical way for Γ-circuit (Fig. 1) as function of slip:

$$M = \frac{3U^2 R\, p\, \omega s}{\left[\left(1+\frac{L_\sigma}{L_1}\right)R_1\, \omega s + \left(1+\frac{R_1}{R_{Fe}}\right)R\,\omega\right]^2 + \left[\left(1+\frac{R_1}{R_{Fe}}\right)\omega^2\, s\, L_\sigma - \frac{R_1\, R}{L_1}\right]^2}, \qquad (1)$$

where M [N.m] is torque, f [Hz] is stator frequence, $\omega = 2\pi f$ [rad.s^{-1}] is angular frequency.

2.2. IDENTIFICATION OF THE EQUIVALENT CIRCUIT PARAMETERS

The identification principle of parameters of equivalent circuit of IM is based on comparing measured input impedance of IM with calculated input impedance of equivalent circuit (Fig. 1). The input impedance is taken in the form of serial combination of the resistance and inductance. The equations for exact parameters identification of the equivalent circuit are derived in [4]. The identification is done for two different points on speed-torque characteristic. The input impedance is calculated from the measured input power, stator voltage and stator current. It is advantageous to measure these values near of nominal point of speed-torque characteristic. The reason lies in the suppression of the skin effect influence on the speed-torque characteristics deformation.

3. THE SKIN EFFECT IN THE SQUIRREL CAGE

Electrical skin effect appears in all alternating current circuits. At this phenomenon AC current is pushed out from conductor centre to its surface. The deep bar effect causes the effective resistance of the conductor to increase with the frequency of the current.

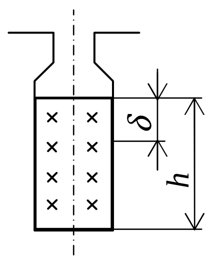

Fig. 2: Illustration of rectangular rotor bar in the rotor slot.

The assumption is that harmonic current with amplitude I and angular frequency $\omega = 2\pi f$ is flowing through rectangular conductor (Fig. 2). Than is possible derived equations describing skin effect in this conductor, see [5].

3.1. THE SKIN DEPTH

The skin depth is the distance at which the current decreases to e^{-1} ≅ 0,3679 of its original value.

$$\delta = \sqrt{\frac{2\rho}{\omega\mu_0}}\,, \tag{2}$$

where δ [m] is skin depth, ρ [Ω.m] is electrical resistivity, μ_0 = 4π 10^{-7} [-] is permeability of vacuum. For aluminium, at the frequency 50 Hz, the skin depth reaches $\delta \cong$ 11,97 mm.

3.2. The Dependence of the bar resistance and bar inductance on frequency

For simplification of the notation it is appropriate to establish a new variable, the reduced conductor high, which is given as the ratio of conductor high and skin depth:

$$\xi = \frac{h}{\delta}, \tag{3}$$

where ξ [-] is reduced conductor high, *h* [m] is conductor high.

Than it is possible to derive the frequency dependence of the bar resistance in the form

$$\varphi_R(\xi) = \frac{R_{AC}}{R_{DC}} = \xi\,\frac{\sinh(2\xi)+\sin(2\xi)}{\cosh(2\xi)-\cos(2\xi)}, \tag{4}$$

where R_{DC} [Ω] is DC resistance, R_{AC} [Ω] is resistance if considering skin effect.

Similarly it is possible to define the frequency dependence of the bar inductance:

$$\varphi_L(\xi) = \frac{L_{AC}}{L_{DC}} = \frac{3}{2\xi}\,\frac{\sinh(2\xi)-\sin(2\xi)}{\cosh(2\xi)-\cos(2\xi)}, \tag{5}$$

Graphic representation of the functions $\varphi_R(\xi)$ and $\varphi_L(\xi)$ is shown in Fig. 3. It is possible to see that the rotor resistance increases and leakage inductance decreases when the conductor high *h* increases.

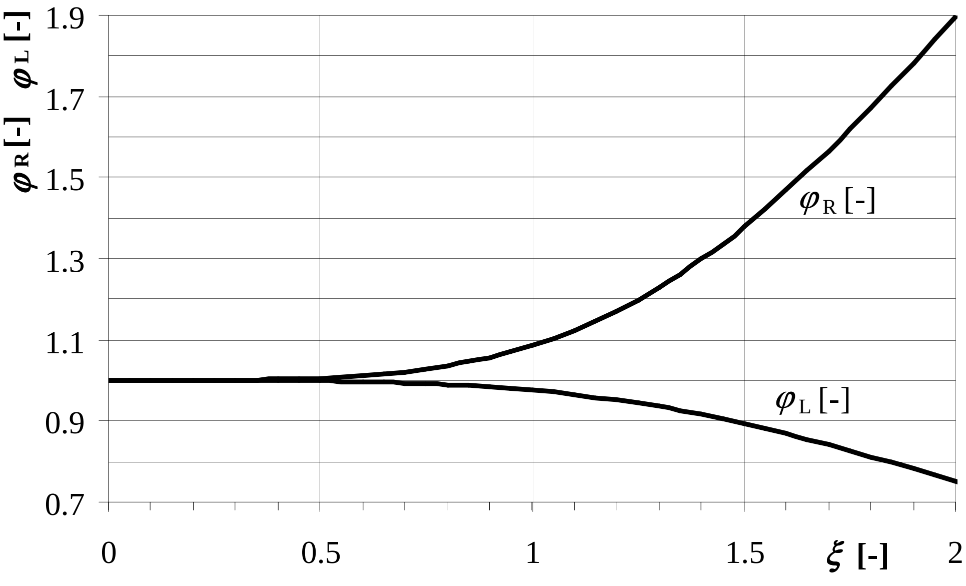

Fig. 3: Functions $\varphi_R(\xi)$ and $\varphi_L(\xi)$.

3.3. THE DEEP BAR EFFECT INFLUENCE ON SPEED-TORQUE CHARACTERISTICS

In Fig. 4, the speed-torque characteristic is shown as the function of rotor frequency at the dependence on conductor high *h* (0 ÷ 20 mm). It is possible to see that the deep bar effect has the totally positive influence on the shape of speed-torque characteristics. But, because of the skin effect influence on the speed-torque characteristic, it is important to do the identification near to nominal point, than it is possible to neglect deep bar effect during identification.

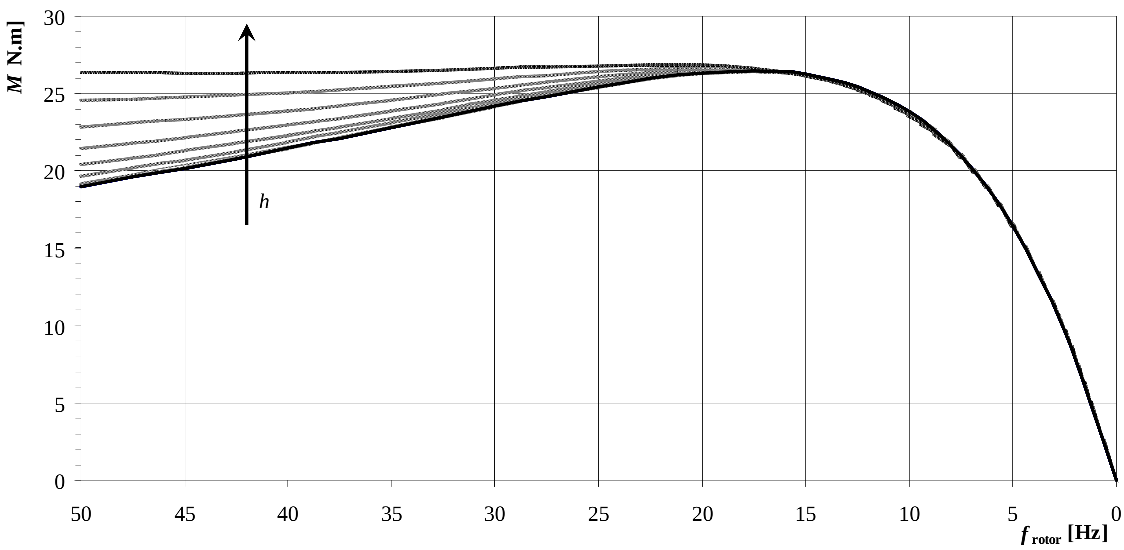

Fig. 4: Calculated speed-torque characteristics of IM when changing the conductor high *h* (0 ÷ 20 mm).

3.4. THE COMPARISON OF MEASURED AND COMPUTED TORQUE CHARACTERISTICS

The measured and the computed speed-torque characteristics are plotted in Fig. 5 for induction motor AOM090L02-016 (2,2 kW, $2p = 2$, 400V Y):

- M1: Measured speed-torque characteristics, using dynamometer.
- M2: Measured speed-torque characteristics, using the dynamic method with the flywheel, see [6].
- M3: Computed speed-torque characteristic, using equation (1).
- M4: Computed speed-torque characteristic, using equation (1) when regarding the skin effect in the rotor bars.

It is necessary to say that characteristics M1 is unsuitable for the following comparison because each point of this characteristic is measured at different temperature. This effect influences of the resistance values.

In the opposition to the M1, the M2 characteristic is measured at the almost constant temperature, because of the very quick measurement.

Computed M3 characteristics deflects from measured M2 at high slips because the skin effect is not taken into account.

Computed M4 characteristics is very well fitted to the measured M2 because of regarding the skin effect.

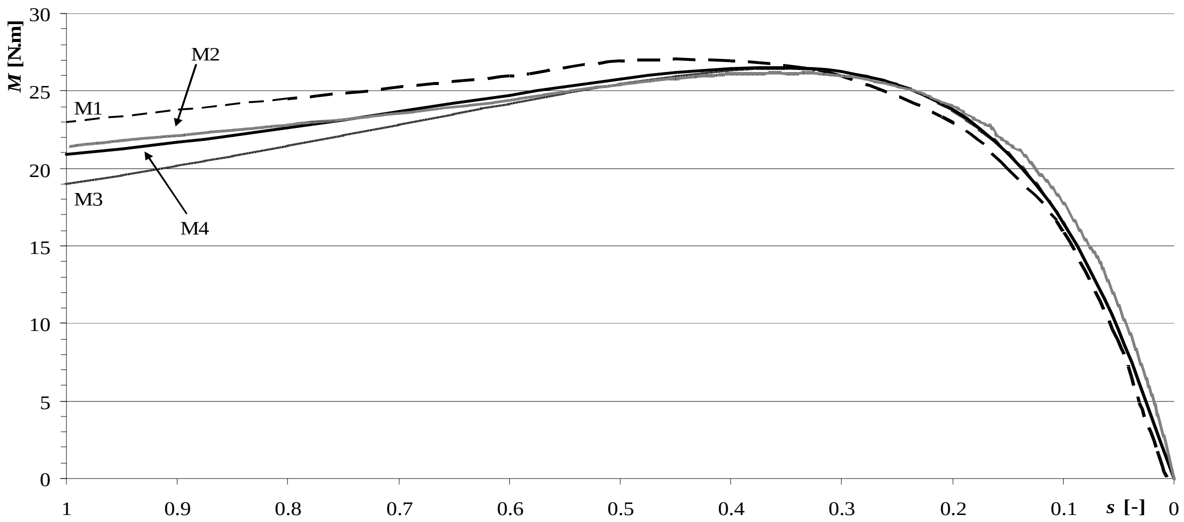

Fig. 5: Comparison of measured and computed speed-torque characteristics.

4. CONCLUSION

The following conclusion appears from the all previous solutions:

- It is possible to use the Γ-circuit, not classical T-circuit, to the torque characteristics calculations.
- But, the accurate correspondence between both, the measured and calculated, characteristics is possible only at following conditions:
- the temperature influence must be eliminated during the measurement (to keep the constant resistance values),
- the skin effect must be considered at the torque characteristics calculations.

ACKNOWLEDGEMENT

This article has been created with the support of the grant no. 102/06/1036 of the grant agency GAČR, and with the support of the grant no. 0021630516 of the MŠMT.

REFERENCES

[1] Patočka M.: Několik poznámek k transformátoru. Sborník konf. SYMEP´04, ČVUT FEL Praha, červen 2004.

[2] Novotny D. W., Lipo T. A.: Vector Control and Dynamics of AC Drives. Oxford University Press Inc., New York, 1996.

[3] Patočka M.: Střídavé stroje. Učební text FEKT VUT v Brně, Verze z 9. 10. 2007.

[4] Běloušek J.: Identifikace parametrů asynchronního motoru, Diplomová práce FEKT VUT v Brně, 2006.

[5] Bašta J., Chládek J., Mayer I.: Teorie elektrických strojů, SNTL, 1968.

[6] Běloušek J., Patočka M.: Dynamická metoda měření momentové charakteristiky asynchronního motoru, Sborník konf. EPVE 08, VUT FEKT Brno, 2008.